

# Performance of the ATLAS muon trigger in $pp$ collisions at $\sqrt{s} = 8$ TeV

MJ Woudstra on behalf of the ATLAS Collaboration

University of Manchester, Oxford Road, Manchester M13 9PL, UK

E-mail: [martin.woudstra@cern.ch](mailto:martin.woudstra@cern.ch)

**Abstract.** Given the harsh detector environment produced by collisions of high energy protons at the LHC, events with muons in the final state are an important signature for many physics analyses. The ATLAS experiment employs a multi-level trigger architecture that selects the events in three sequential steps of increasing complexity and accuracy. The Level 1 trigger is implemented with custom-built hardware to reduce the event rate (in 2012) from 20 MHz to 70 kHz. Then the software-based higher level triggers refine the trigger decisions reducing the output rate down to several 100 Hz. The performance of the muon trigger is presented as determined with  $pp$  collision data collected in 2012 at a centre-of-mass energy of 8 TeV.

## 1. Introduction

Muons in the final state are distinctive signatures of many physics studies performed at the LHC, such as the observation and measurements of a Higgs boson, searches for new phenomena, as well as the measurements of Standard Model (SM) processes. The ATLAS muon trigger system has been designed to select muons in a wide momentum range with high efficiency. The precise determination of the muon trigger performance of the ATLAS detector [1] at the LHC is essential for muon-related physics analyses. The ATLAS experiment collected  $pp$  collision data in 2012 at a center-of-mass energy of 8 TeV with maximum instantaneous luminosity of  $7.7 \times 10^{33} \text{ cm}^{-2} \text{ s}^{-1}$ . To address a wide variety of physics topics, the ATLAS experiment deployed several muon triggers. Here we present results on the general purpose high- $p_T$  single muon triggers, and medium- $p_T$  di-muon triggers for used for SM processes and for searches.

## 2. The Muon trigger

The trigger system [2] selects events with muons in three steps. The first step uses fast-response trigger chambers and custom-built hardware to generate a L1 trigger based on hit coincidences. The second and third step make up the High Level Trigger (HLT), and are software based.

The ATLAS muon spectrometer (MS) [3] is the outermost detector and surrounds the calorimeter system. The MS both identifies muons and measures their momentum and position up to pseudo-rapidity  $|\eta| = 2.7$ . The magnetic field in the MS is provided by three large air-core superconducting toroidal magnet systems (two endcaps and one barrel) providing an average field of approximately 0.5 T. Figure 1 shows a quarter longitudinal section of the MS. The deflection of the muon trajectories in the magnetic field is measured using hits in three layers of precision drift tube (MDT) chambers for  $|\eta| < 2.0$ . For  $\eta$  in the region  $2.0 < |\eta| < 2.7$ , two layers of MDT chambers and one layer of cathode strip chambers (CSC) are used. Three layers



of resistive plate chambers (RPC) in the barrel region ( $|\eta| < 1.05$ ) and three layers of thin gap chambers (TGC) in the endcap regions ( $1.05 < |\eta| < 2.4$ ) provide the L1 muon trigger.

The ATLAS inner detector (ID) [4] measures tracks up to  $|\eta| = 2.5$  in a solenoidal magnetic field of 2 T. The momenta and positions of the muons are measured independently in the ID and in the MS, and the ID-MS combination provides the most precise measurement of the muon kinematics, as well as the lowest fake rate.

### 2.1. Level-1 muon trigger

The L1 muon trigger identifies candidates by a coincidence of hits in 2 layers (“low  $p_T$ ”) or 3 layers (“high  $p_T$ ”) of trigger chambers (see figure 1). The L1 trigger carries information on the detector region where the muon passed (the “Region of Interest” or RoI). It also estimates the  $p_T$  of the muon by looking at the degree of deviation of the hit pattern from a straight line. The  $p_T$  is classified according to a set of pre-defined thresholds indicated by labels like MU15 (for  $p_T > 15$  GeV). MU10 and lower are “low  $p_T$ ” triggers, and MU11 and higher are “high  $p_T$ ” triggers. The geometrical coverage of the L1 trigger is about 99% in the end-cap regions and about 80% in the barrel region.

The lower coverage in the barrel region is due to a crack at around  $|\eta| = 0$  (for services to the ID and calorimeters), the feet of the ATLAS detector and two elevators in the bottom part of the MS. The high  $p_T$  triggers in the barrel region have about 6% lower efficiency than the low  $p_T$  triggers due to the requirement of the 3<sup>rd</sup> layer in the coincidence [5].

### 2.2. High Level muon trigger

The HLT RoI-based triggers only look in the region of the detector indicated by the L1 RoI, therefore reducing the amount of data to be transferred and processed. The Level 2 (L2) muon trigger is software based and uses dedicated fast muon reconstruction algorithms, and only uses detector data around the RoI. The Event Filter (EF) muon software trigger leverages the precise offline muon reconstruction algorithms, and has access to the data of the full detector.

L2 and EF follow the same basic strategy: first they reconstruct a “standalone” muon track using only the data from the MS (trigger chambers *and* precision chambers). This track is then combined with a track in the ID to form a “combined” muon. At EF, there is an additional algorithm which starts with ID tracks around the L1 RoI and extrapolates those to the muon detectors to collect the data from the MS either to form a combined muon candidate or to just tag the ID track as a muon. These two strategies were run in parallel until the end of the 2011 run, but from 2012 onwards they were combined to save CPU time. The former algorithm is run first and the latter algorithm is run only if the first one does not find a muon candidate, giving the highest efficiency with optimal CPU time [5].

To allow for a lower  $p_T$  threshold while keeping the trigger rate under control, isolation is added as an extra requirement to the muon candidate. The isolation algorithm sums the  $p_T$  of all ID tracks ( $p_T > 1$  GeV) in a cone with  $\Delta R = 0.2$  centered around the muon candidate. It subtracts the  $p_T$  of the muon and then divides by the  $p_T$  of the muon to get the relative track isolation. The isolation requirement was introduced in the main single-muon trigger in 2012.

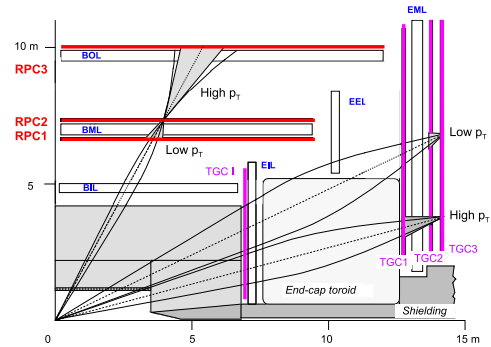


**Figure 1.** Quarter longitudinal section of the muon system. The curved lines represent muon tracks. Low  $p_T$  triggers require a coincidence between 2 layers of trigger chambers, and high  $p_T$  triggers between 3 layers, as indicated. BIL, BML, BOL, EIL, EEL and EML are locations of MDT chambers.

2.3. Primary muon triggers in 2012

Primary muon triggers are general-purpose triggers that were not pre-scaled during the whole of 2012 running. They are summarized in table 1.

**Table 1.** Primary muon triggers in 2012 running.

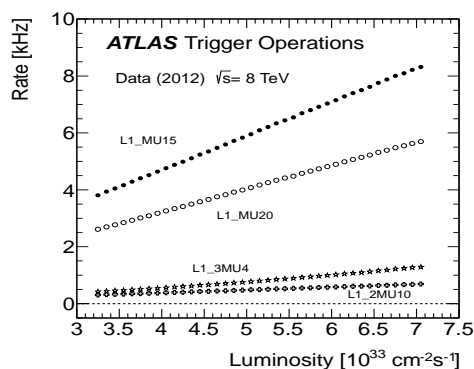
Trigger name	Level 1	Level 2	Event Filter
mu24i	MU15	$p_T > 22$ GeV	$p_T > 24$ GeV, $\Sigma^{\Delta R < 0.2} p_T^{trk} / p_T^\mu < 0.12$
mu36	MU15	$p_T > 22$ GeV	$p_T > 36$ GeV
mu40_SA_barrel	MU15	$p_T > 40$ GeV, $ \eta  < 1.05$	$p_T > 40$ GeV, $ \eta  < 1.05$
2mu13	2MU10	2 $\mu$ 's with $p_T > 13$ GeV	2 $\mu$ 's with $p_T > 13$ GeV
mu18_mu8_FS	MU15	1 $\mu$ with $p_T > 18$ GeV	2 $\mu$ 's with $p_{T,1}^{FS} > 18$ GeV, $p_{T,2}^{FS} > 8$ GeV

The mu24i trigger selects isolated muons with  $p_T > 25$  GeV and a relative track isolation of  $< 0.12$ . The mu36 trigger is designed to collect muons with large  $p_T$  without bias due to any isolation requirement. The mu40\_SA\_barrel trigger decision is based only on MS reconstruction, active only in the barrel region because of the high rate in the endcap regions.

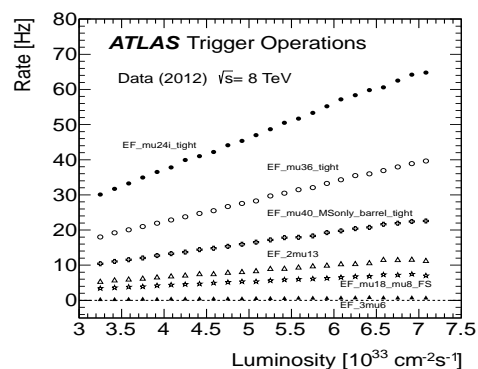
Physics analyses requiring muon triggers with lower  $p_T$  thresholds use either multi-muon triggers or muon triggers in combination with other triggers (electron, jet, missing  $E_T$ , ...). Multi-muon triggers are made by requiring multiple single-muon triggers (such as 2mu13, which has at least 2 mu13 triggers). The “full-scan” algorithm finds multiple muons by scanning the full detector in the EF once the leading  $p_T$  single muon trigger has fired. This method is less affected by the low muon barrel L1 geometrical efficiency. The full-scan trigger mu18\_mu8\_FS requires a leading muon with  $p_T > 18$  GeV and a second muon at the EF with  $p_T > 8$  GeV.

3. Muon trigger rates

Figures 2 and 3 show the L1 and EF trigger rates as a function of the instantaneous luminosity in the 2012 runs, for the primary muon triggers. The trigger rates scale linearly with the instantaneous luminosity.



**Figure 2.** L1 muon trigger rates [5].



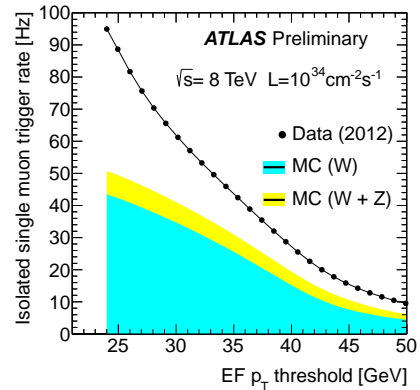
**Figure 3.** EF muon trigger rates [5].

Figure 4 shows the isolated trigger rate as a function of the  $p_T$  threshold for tracks reconstructed by the EF. The rate is normalized to an instantaneous luminosity of  $1 \times 10^{34} \text{ cm}^{-2} \text{ s}^{-1}$ . Figure 4 also shows  $W \rightarrow \mu\nu$  and  $Z \rightarrow \mu\mu$  contributions as expected from MC, normalized according to their MC predicted cross sections. At threshold  $p_T = 24$  GeV about half of the triggered muon events are due to muons from  $W$ 's and  $Z$ 's. The contributions from  $W$ 's and  $Z$ 's dominate for thresholds  $p_T > 40$  GeV.

#### 4. Muon trigger efficiencies in 2012

##### 4.1. Efficiency measurement with $Z$ tag-and-probe method

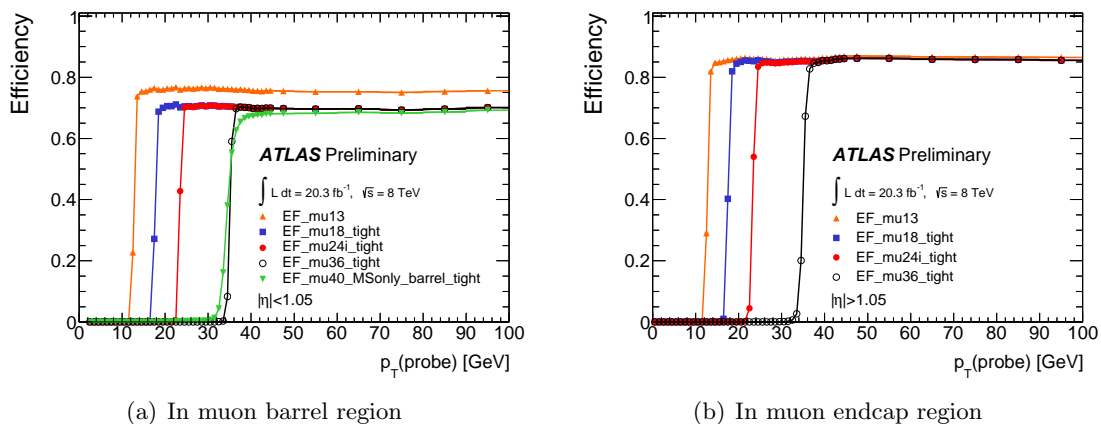
The efficiencies are measured in-situ with  $pp$  collision events using the tag-and-probe method on candidate  $Z \rightarrow \mu\mu$  events. These are selected by requiring a pair of oppositely charged offline reconstructed muons with a dimuon invariant mass within 10 GeV of the mass of the  $Z$  boson. Both muons must be isolated with a relative track isolation in a cone of 0.2 of less than 0.1. The tag muon must have in addition  $p_T > 25$  GeV and it must match a trigger muon that has passed either the mu24i or mu36 trigger. The probe muon is the other muon in the pair. The efficiency of a particular muon trigger is then defined as the fraction of probe muons that can be matched to that trigger muon.



**Figure 4.** Projected rate for isolated trigger at an instantaneous luminosity of  $1 \times 10^{34} \text{ cm}^{-2} \text{ s}^{-1}$ , as a function of the  $p_T$  threshold [5].

##### 4.2. Efficiencies of primary single-muon triggers in 2012

Figure 5 shows the turn-on curves of the primary muon triggers. In the barrel region the plateau efficiency of mu13 is about 6% higher than other triggers. This is because mu13 is seeded from a low  $p_T$  L1 trigger (MU10), while the other triggers are seeded from a high  $p_T$  L1 trigger (MU15). See section 2.1 for low  $p_T$  vs. high  $p_T$  trigger.



(a) In muon barrel region

(b) In muon endcap region

**Figure 5.** Efficiency measured as a function of the probe muon  $p_T$  for mu13, mu18, mu24i, mu36 and mu40\_MSonly\_barrel. The error bars indicate statistical uncertainties only [5].

The turn on curve of mu40\_MSonly\_barrel is much slower than the other triggers. This is because mu40\_MSonly\_barrel only uses the measurements of muon detectors, so the  $p_T$  resolution is worse.

The OR between mu36 and mu40\_MSonly\_barrel results in 1.5 – 2% higher efficiency in the barrel region. Therefore, mu36 OR mu40\_MSonly\_barrel is considered as the primary single muon trigger for physics analyses focusing on processes that include muons with  $p_T > 50$  GeV, for example searches for exotic bosons  $W'$  and  $Z'$ .

The plateau's of the measured efficiencies of mu24i and mu36 are the same. However, since this efficiency is measured with respect to *isolated* offline muons, taking the OR between these two is considered the primary single-muon trigger for general physics analyses, to keep high efficiency also for non-isolated muons at high  $p_T$ . Figure 6 shows the measured efficiency of this primary single-muon trigger in the barrel and endcap regions. The plateau efficiency is about

70% in the barrel and 86% in the endcap regions. The efficiency turns on sharply around the threshold, reaching a plateau already around  $p_T \simeq 25$  GeV.

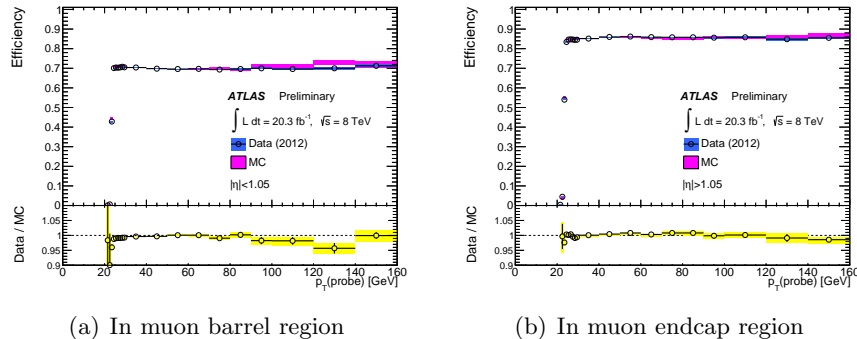


**Figure 6.** Efficiencies of mu24i OR mu36 triggers as functions of the probe muon  $p_T$ . Open circles and open triangles show data and MC, respectively. The lower part of each plot shows the ratio of data efficiencies to those of MC [5].

Figure 7 shows the measured efficiency of mu24i OR mu36 separately for trigger levels L1, L2 and EF. Each higher trigger level has a sharper turn-on than the previous level. The plateau efficiency is dominated by L1. The HLT efficiency with respect to the L1 is about 98 – 99%.

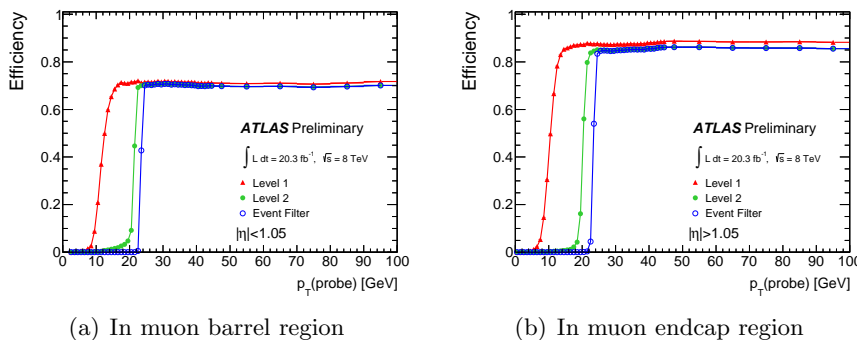


**Figure 7.** Efficiencies of mu24i OR mu36 triggers as functions of the probe muon  $p_T$ , separately for trigger levels: Level 1, Level 2 and Event Filter [5].

## 5. Conclusion and prospects

The ATLAS muon trigger has performed very well in 2012. During the LHC shutdown the trigger is being upgraded, both on the hardware side and the software side, to be ready for an excellent performance in the much harsher conditions expected for the restart in 2015.

## References

- [1] ATLAS Collaboration, The ATLAS experiment at the CERN Large Hadron Collider, *JINST* **3**, S08003 (2008) 1–437.
- [2] ATLAS Collaboration, Performance of the ATLAS Trigger System in 2010, *Eur.Phys.J.* **C72** (2012) 1849
- [3] ATLAS Collaboration, Preliminary results on the muon reconstruction efficiency, momentum resolution, and momentum scale in ATLAS 2012  $pp$  collision data, ATLAS-CONF-2013-088, <http://cds.cern.ch/record/1580207/>
- [4] ATLAS Collaboration, The Expected Performance of the ATLAS Inner Detector, ATL-PHYS-PUB-2009-002, <http://cds.cern.ch/record/1118445/>
- [5] <https://twiki.cern.ch/twiki/bin/view/AtlasPublic/MuonTriggerPublicResults>